Electron diffraction
Masatsugu Sei Suzuki
Department of Physics, SUNY at Binghamton
(Date: February 04, 2018)

Unlike other types of radiation used in diffraction studies of materials, such as x-rays and neutrons, electrons are charged particles and interact with matter through the Coulomb forces. This means that the incident electrons feel the influence of both the positively charged atomic nuclei and the surrounding electrons. In comparison, x-rays interact with the spatial distribution of the valence electrons, while neutrons are scattered by the atomic nuclei through the strong nuclear forces. In addition, the magnetic moment of neutrons is non-zero, and they are therefore also scattered by magnetic fields. Because of these different forms of interaction, the three types of radiation are suitable for different studies
https://en.wikipedia.org/wiki/Electron_diffraction

Clinton Joseph Davisson (October 22, 1881 – February 1, 1958), was an American physicist who won the 1937 Nobel Prize in Physics for his discovery of electron diffraction. Davisson shared the Nobel Prize with George Paget Thomson, who independently discovered electron diffraction at about the same time as Davisson.

http://en.wikipedia.org/wiki/Clinton_Joseph_Davisson

Sir George Paget Thomson, FRS (3 May 1892 – 10 September 1975) was an English physicist and Nobel laureate in physics recognised for his discovery with Clinton Davisson of the wave properties of the electron by electron diffraction.

http://en.wikipedia.org/wiki/George_Paget_Thomson

LEED	(low energy electron diffraction) is a technique for the determination of the surface structure of crystalline materials by bombardment with a collimated beam of low energy electrons (20 - 200 eV) and observation of diffracted electrons as spot on the fluorescent screen. This experiment can be performed in an ultra-high-vacuum environment.
RHEED	(reflection high-energy electron diffraction) is a technique used to characterize the surface of crystalline materials. RHEED systems gather information only from the surface layer of the sample.

1. Introduction

The low energy electrons are absorbed before they have penetrated more than a few atomic layers. The LEED can be performed in a reflection mode. It can be used to determine the several atomic layers of a single crystal. The first electron diffraction experiment was performed by Davisson and Germer in 1927, and demonstrated the wave-nature of electrons. The atomically cleaned surfaces state of the system is essential to this experiment. The experiment can be performed in ultra high vacuum ($p<10^{-8}$ Pa). See the detail of de Broglie wave and Davisson-Germer experiment on the Lecture Note of Modern Physics (Phys.323):

http://bingweb.binghamton.edu/~suzuki/ModernPhysics.html

2. de Broglie wave length of electron

We consider the de Broglie wavelength of a particle *m* and the kinetic energy *K* for a relativistic particle.

$$E = \sqrt{E_0{}^2 + c^2 p^2} = E_0 + K ,$$

where E_0 is the rest energy;

$$E_0 = mc^2$$

The kinetic energy *K* is

$$K = E - E_0 = \sqrt{E_0{}^2 + c^2 p^2} - E_0 .$$

Then the momentum *p* is obtained as

$$p = \frac{1}{c}\sqrt{\left(K + E_0\right)^2 - E_0{}^2} = \frac{1}{c}\sqrt{K^2 + 2KE_0} = \frac{1}{c}\sqrt{K(K + 2E_0)} .$$

Using the de Broglie relation, we have the de Broglie wavelength

$$\lambda = \frac{h}{p} = \frac{hc}{\sqrt{K\left(K + 2E_0\right)}} .$$

We find that the wavelength is a scaling function of K/E_0 as

$$\lambda = \frac{\frac{hc}{E_0}}{\sqrt{\frac{K}{E_0}\left(\frac{K}{E_0} + 2\right)}} .$$

We consider the case of electron. In this case, the above formula is

$$\frac{\lambda}{\lambda_c} = \frac{1}{\sqrt{\frac{K}{E_0}\left(\frac{K}{E_0} + 2\right)}} .$$

Note that λ_c is the Compton wavelength for the particle and is given by

$$\lambda_c = \frac{h}{mc} = 2.4263102389\times10^{-12} \text{ m.}$$

for the electron.

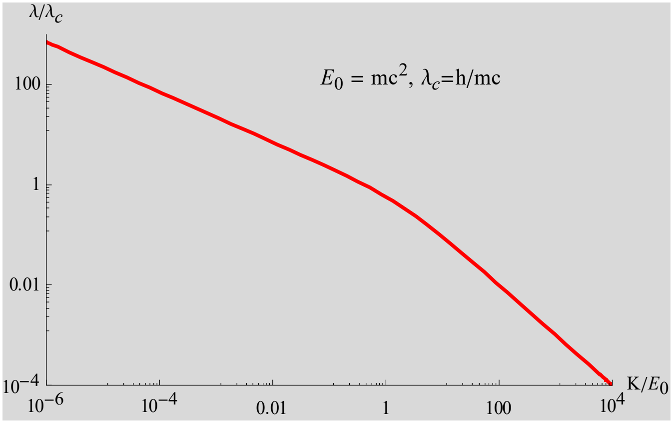

The nonrelativistic case.
When $E_0 >> K$, λ can be approximated by

$$\lambda = \frac{h}{p} = \frac{hc}{\sqrt{2KE_0}} = \frac{hc}{\sqrt{2Kmc^2}} = \frac{h}{\sqrt{2mK}}$$

or

$$\lambda_{classical} = \frac{h}{\sqrt{2mK}}$$

3. Electron: Classical limit

The de Broglie wavelength (relativistic) vs the kinetic energy for electron

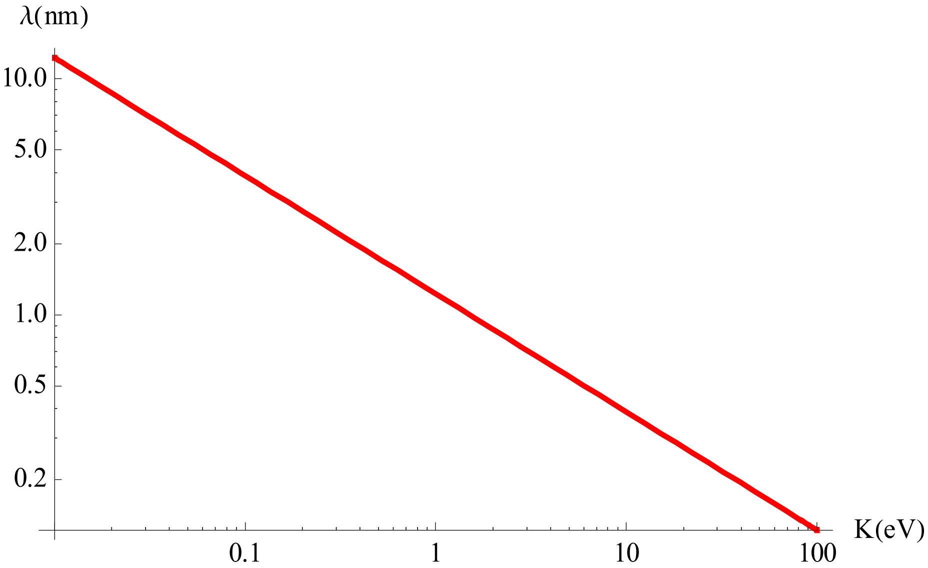

Fig. The plot of the wavelength (classical) of electron as a function of the kinetic energy *K*(eV).

In the nonrelativistic case,

$$\boxed{\lambda_{classical} = \frac{12.2643}{\sqrt{K(eV)}} \text{Å}}$$

When K = 100 eV, the wavelength is λ = 1.22643 Å. When K = 100 keV, the wavelength is λ = 0.03878 Å and the wavenumber k is 162 Å^{-1}.

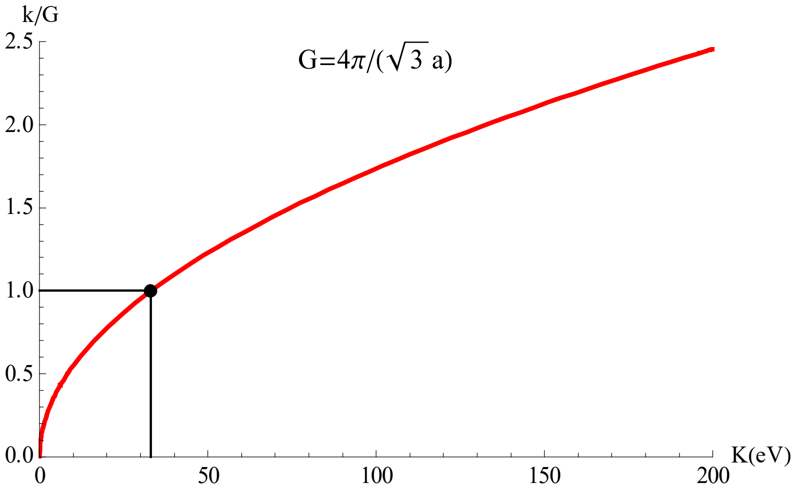

Fig. The ratio of the radius of Ewald sphere ($k = 2\pi/\lambda$) to the in-plane reciprocal lattice wavenumber for the graphite. $G = \dfrac{4\pi}{\sqrt{3}a} = 2.95$ Å^{-1}. $a = 2.46$ Å (lattice constant of graphite layer). At $K = 33.1401$ eV, $k/G = 1$.

Figure shows the plot of the ratio of the radius of Ewald sphere ($k = 2\pi/\lambda$) to the reciprocal lattice wavenumber for the graphite (as an example), as a function of the kinetic energy of electron, K (eV).; $G = \dfrac{4\pi}{\sqrt{3}a} = 2.95$ Å^{-1} with $a = 2.46$ Å (in-plane lattice constant). This ratio k/G increases with increasing the kinetic energy of K. The ratio is equal to 1 when $K = 33.1401$ eV.

4. Numerical calculation of the wave length

E_0 is the rest mass of electron and is given by

$$E_0 = mc^2 = 510.999 \text{ keV} = 0.510999 \text{ MeV}.$$

The wavelength of electron (relativistically) is given by

$$\lambda_{relativistic} = \frac{0.548474}{\sqrt{[2 + 0.00195695K(keV)]K(keV)}} \quad (\text{Å})$$

for the high energy limit of electron, and

$$\lambda_{classical} = \frac{12.2643}{\sqrt{10^3 K(keV)}} \quad (\text{Å})$$

classically (for the low energy limit), where K is the kinetic energy in the units of keV.

K (keV)	$\lambda_{classical}$ (Å)	$\lambda_{relativistic}$ (Å)
0.01	3.87831	3.87828
0.1	1.22643	1.22637
1	0.387831	0.38764
10	0.122643	0.122047
100	0.0387831	0.0370144

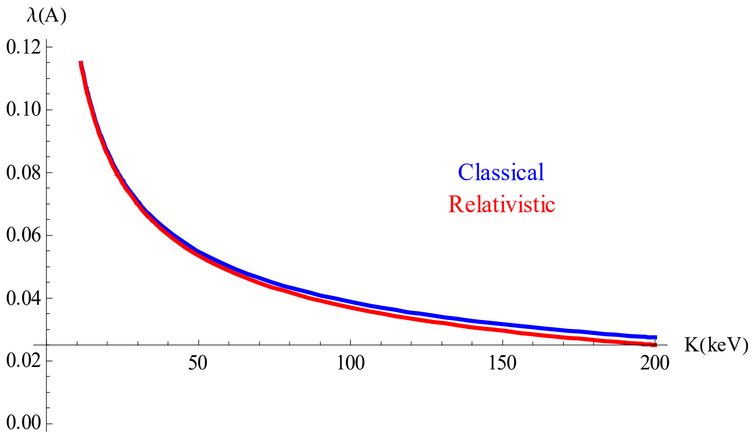

Fig. The plot of the wavelength of electron as a function of the kinetic energy K (keV). $\lambda_{relativistic}$ (red line) is slightly shorter than $\lambda_{classical}$ (blue line).

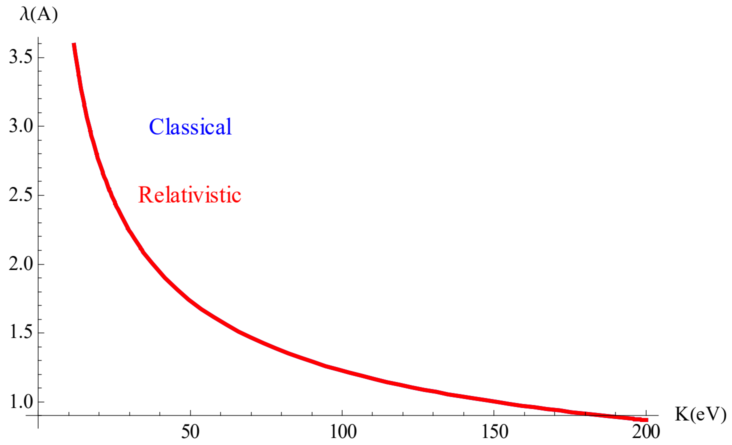

Fig. The plot of the wavelength of electron as a function of the kinetic energy K (eV). $\lambda_{relativistic} \approx \lambda_{classical}$. The red and blue lines are completely overlapped.

5. LEED experiment

The LEED experiment uses a beam of electrons of a well-defined low energy (typically in the range 20 - 200 eV) incident normally on the sample. The sample itself must be a single crystal with a well-ordered surface structure in order to generate a back-scattered electron diffraction pattern.

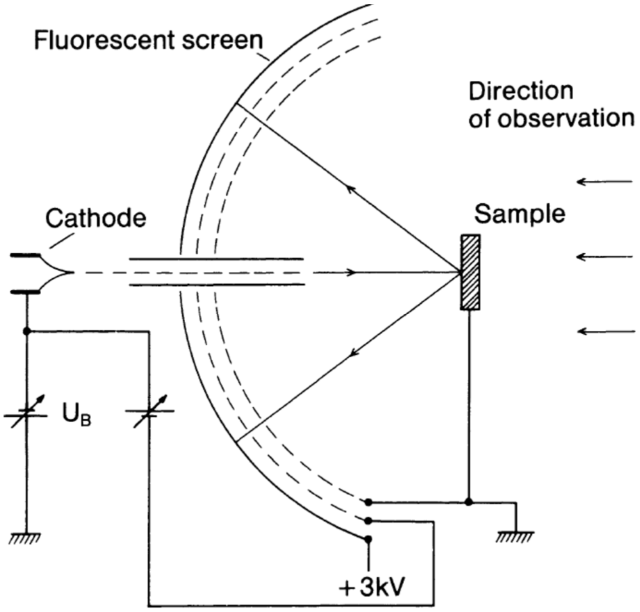

Fig. Schematic of the experimental arrangement used to observe LEED reflections from the surface of a single crystal.

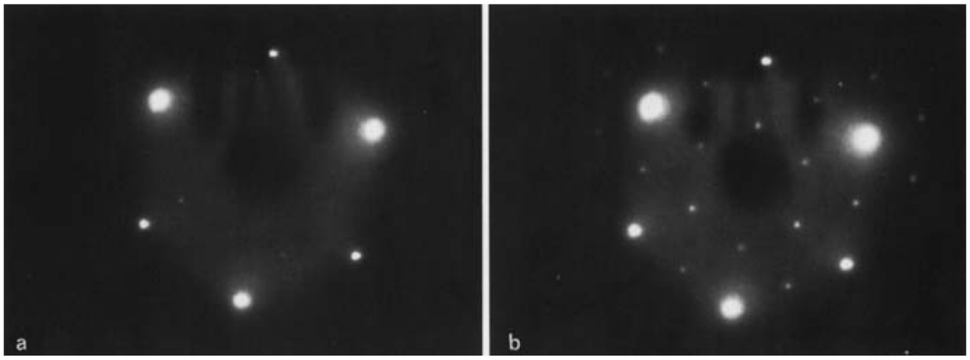

Fig. (a) LEED diffraction pattern from a Ni (111) surface at a primary electron energy of K = 205 eV (λ = 0.86 Å). (b) The LEED diffraction patter observed after the adsorption of hydrogen. The extra spots indicates the formation of a (2x2) adsorbate superlattice.
(H. Ibach and H. Lűth, Solid-State Physics, 4th edition (Springer, Berlin, 2009), p.73.

geometrical condition to be satisfied is that the surface of a sphere intersect a collection of *rods,* as in Fig. This condition is guaranteed to be satisfied at some scattering angles for any choice of incoming wave vector *ko* and for any orientation of the sample, in contrast with the bulk case. There is no need to rotate the sample, scan through incoming wave vectors, or use powdered samples in order to obtain scattering peaks.

Despite LEED's crucial historical role in demonstrating the wave nature of the electron, it is not easy to determine detailed features of surfaces based upon LEED measurements. Because electrons interact very strongly with solids, multiple scattering is impossible to avoid. Quantitative comparison of theory and experiment requires one to make detailed guesses about surface structure and then carry out lengthy quantum-mechanical calculations for the scattering of electrons from the surfaces, based upon the guesses.

5. Construction of Ewald sphere (LEED): principle

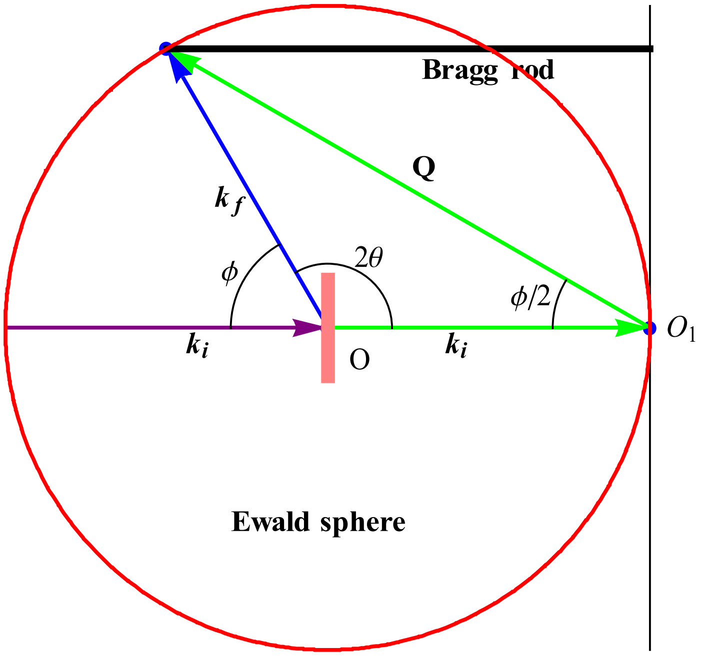

We now consider the Bragg reflections in the 2D system. These Bragg reflections occurs along a reciprocal rod in the reciprocal lattice space. The Bragg peaks appear along the reciprocal rod, which is described by $(\mathbf{G}_{\perp}, \boldsymbol{G}_{//})$. Note that $\mathbf{G}_{\perp}$ is the in-plane reciprocal lattice vector and $G_{//}$ is the out-of-plane wavevector. The incident electron wave ($\boldsymbol{k}_{\mathrm{i}} = \boldsymbol{k}$, $k = 2\pi/\lambda$) is reflected by the surface of the 2D system. $\boldsymbol{k}_{\mathrm{f}}$ (= $\boldsymbol{k}'$) is the wavevector of the out-going electron wave ($k' = 2\pi/\lambda$). The Ewald sphere is formed of the sphere with the radius of $k = k'$. The scattering vector $\boldsymbol{Q}$ is defined by

$$\mathbf{Q} = \mathbf{k}' - \mathbf{k}\,.$$

O_1 is the origin of the reciprocal lattice space. The 2D system is located at the point O. The direction normal to the surface of the system is antiparallel to the direction of the incident electron wave. Since the system is two-dimensional, the reciprocal lattice space is formed of Bragg rods. The Bragg reflections occur when the Bragg rods intersect the Ewald sphere.

((**Note**))

Suppose that the kinetic energy of electron *K* is much larger than 33 eV. The radius of the Ewald sphere is much larger than the separation between adjacent Bragg rods. The Bragg rods intercep with the nearly flat Ewald sphere.

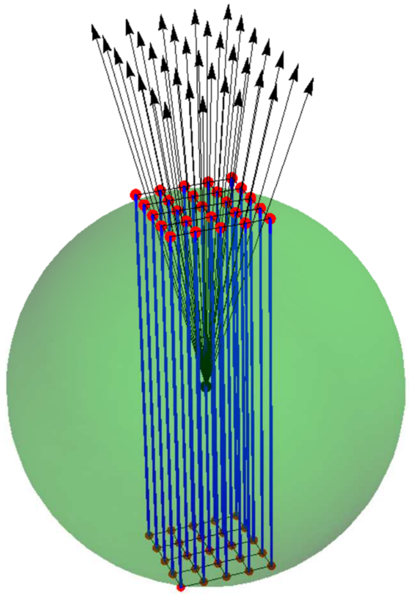

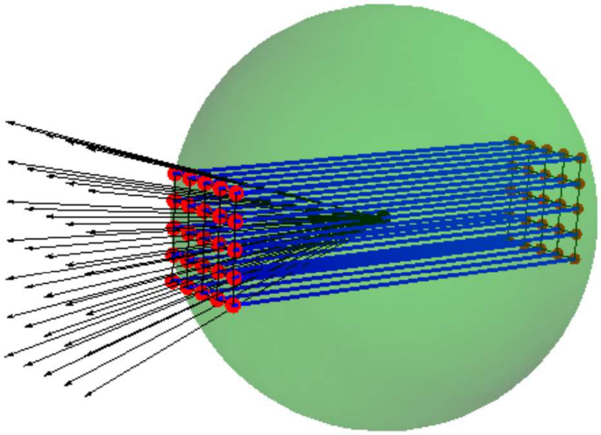

Fig. Construction of the Ewald sphere for the 2D system with square lattice. The Blue lines are reciprocal rods. The black lines denote the direction of the reflected beams. The above two figures are the essentially the same.

6. Ewald sphere for the graphite (LEED)

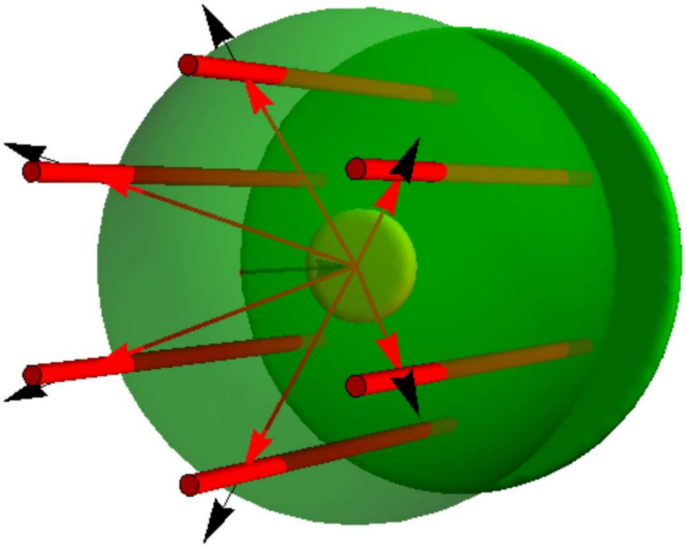

Fig. Construction of the Ewald sphere for the 2D system with square lattice. The reciprocal rods intersect with the Ewald sphere, which leads to the appearance of the Bragg reflections.

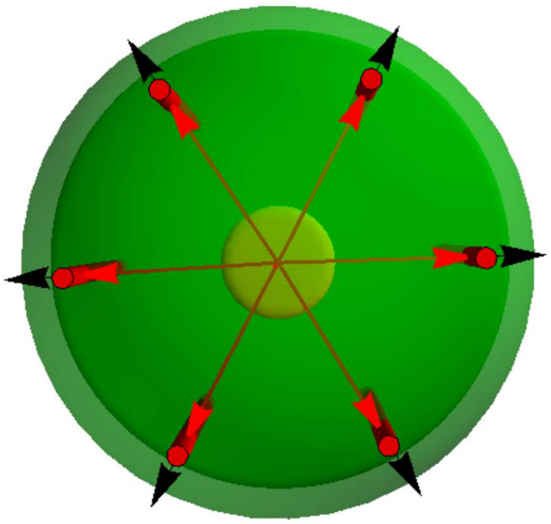

Fig. Construction of the Ewald sphere for the 2D system with hexagonal lattice (view point is different from the above figure).

7. RHEED experiment

In RHEED, the electron beam (is incident at a very grazing angle. In a RHEED experiment, with the sample viewed edge-on. In practice the display screen is usually a phosphor coating on the inside of a vacuum window (viewport) and the diffraction pattern can be viewed and recorded from the atmospheric side of the window. The small scattering angles involved are compensated for by using relatively large sample/screen distances.

Ewald construction for RHEED

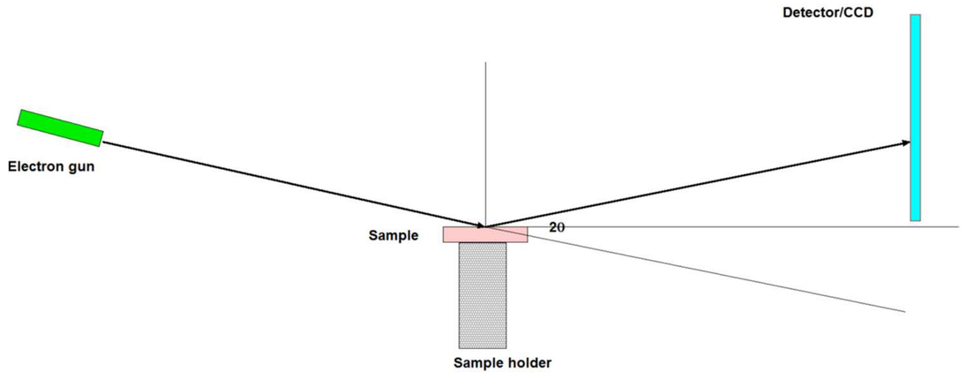

Fig. RHEED experiment, consisting of the electron gun, sample and detector /CCD components of a RHEED system.

Electrons follow the path indicated by the arrow and approach the sample at angle θ. The sample surface diffracts electrons, and some of these diffracted electrons reach the detector and form the RHEED pattern. The reflected (specular) beam follows the path from the sample to the detector. RHEED is based on the reflection of electrons with high kinetic energy (typically in the 5-100 keV) and low impact angle θ (typically less than 5°) from the surface of a solid.

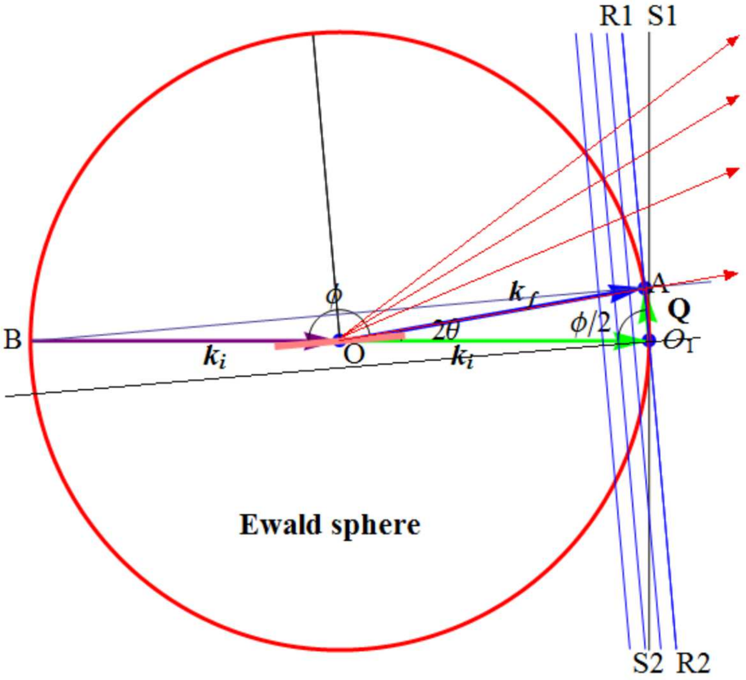

Fig. Ewald construction for the RHEED experiment.

In the Fig. the *a*-*c* plane of the sample is shown, where *c* is the axis perpendicular to the suface and *a* is one of the specified axis inside the surface. O_1 is the origin of the reciprocal lattice space. For the 2D system, the Bragg reflections form reciprocal rod with the in-plane reciprocal lattice G_a. The scattering vector is given by $\overrightarrow{O_1A} = \boldsymbol{Q} = k' - k$. The line R_1R_2 is the reciprocal rod with $G_a = 0$. This line intersects the Ewald sphere at the point A. The reciprocal rods with different G_a are parallel to the line R_1R_2. These rods (blue lines) also intersect with the Ewald sphere, satisfying the Bragg condition. The red lines denote the direction of the outgoing waves. The line S_1S_2 is tangential to the Ewald sphere at the point O_1. When 2θ is very small, the line S_1S_2 is almost parallel to the line R_1R_2.

8. In-plane structure and reciprocal lattice of graphite and graphite intercalation compounds

Here we consider the superstructures observed in the graphite intercalation compounds (GIC's). In alkali metal GIC, alkali metal (AM) atoms are intercalated between the adjacent graphite layers, forming a AM-superstructure. The in-plane structure of AM layers depends on the species of AM atoms, stage number, and so on. The LEED pattern coincides with the superposition of in-reciprocal lattice vectors of AM layers and graphite layers.

(i) C_6Ca is a stage-1 compound (showing superconductivity at low temperatures, recently discovered). The Ca layer form a $p(\sqrt{3}\times\sqrt{3})R0^\circ$ structure. This superstructure is commensurate with the graphite lattice. Ca atoms are located on the hexagon centers.

(ii) C_8K, C_8Rb, and C_8Cs are stage 1 compounds. These AM layers form a $p(2\times 2)R0^\circ$, which is commensurate with the graphite lattice.

(iii) $C_{14}M$. There is no AM GIC having this stoichiometry. However, if it is possible, this M layer is expected to form a $p(\sqrt{7}\times\sqrt{7})R19.11^\circ$, which is also commensurate with the graphite lattice. The M layer is rotated by 19.11° with respect to the graphite layer.

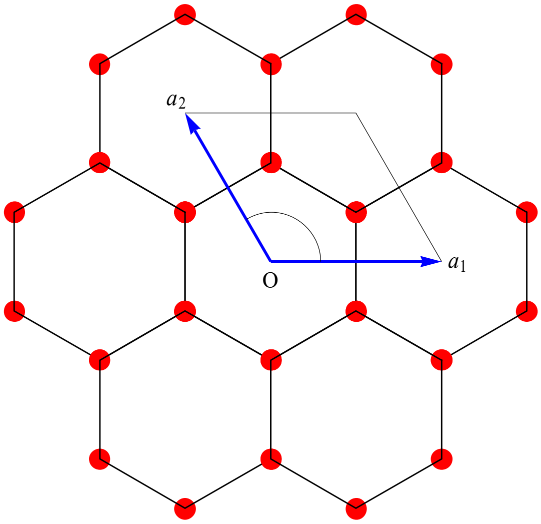

Fig. In-plane structure of graphite layer. $\boldsymbol{a}_1$ and $\boldsymbol{a}_2$ are the primitive translation vectors.

(i) p(1 x 1)R0° structure

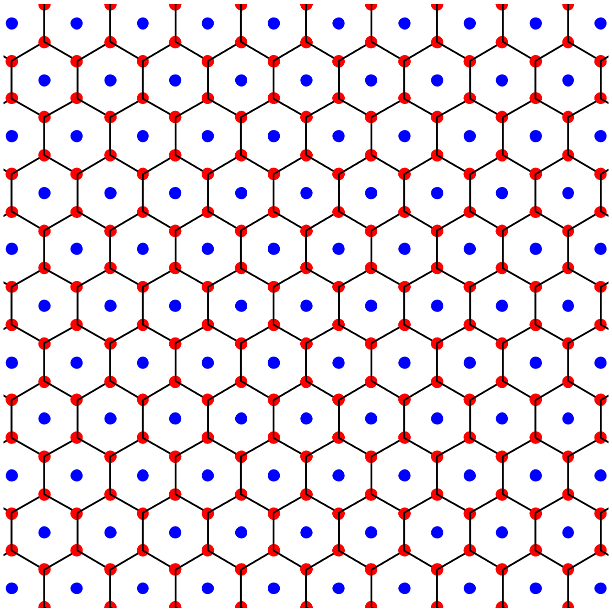

Fig. Schematic diagram of an in-plane unit cell for the p(1 x 1)R0° structure showing the carbon atoms (denoted by red circles) at the corners of the hexagons and the intercalants as the blue circles. *p* denotes the primitive cell. R denotes the rotation between the primitive translation vectors of carbon atoms and intercalant atoms.

(ii) p(2 x 2)R0° structure

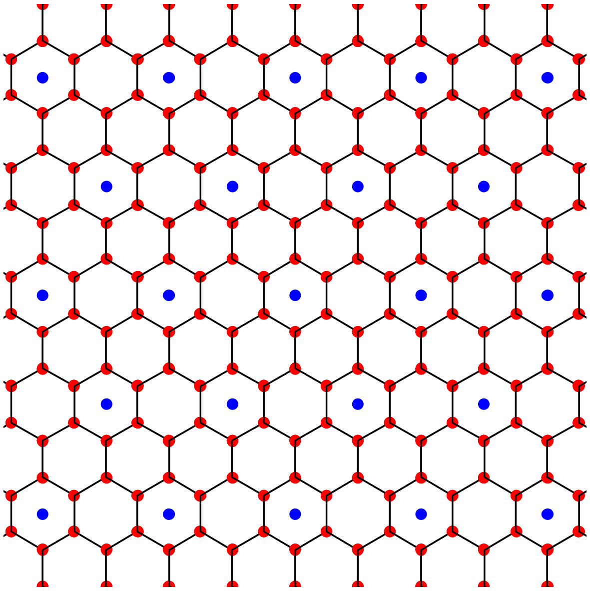

Fig. Schematic diagram of an in-plane unit cell for the p(2 x 2)R0° .

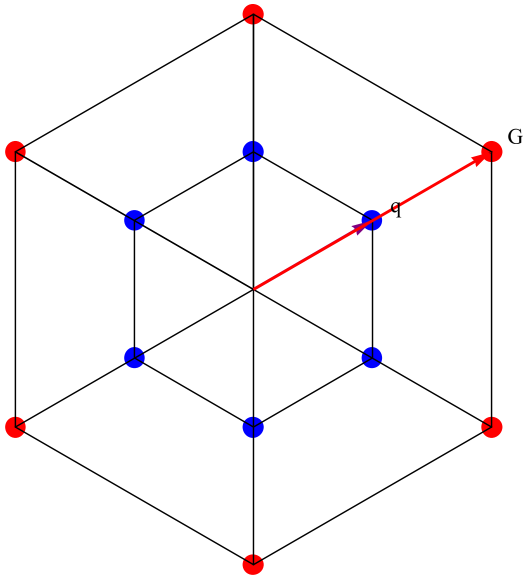

Fig. Bragg reflections arising from the graphite layer (red circles) and intercalate layer (blue circles). The in-plane structure of the intercalate layer is p(2 x 2)R0°.

(iii) p($\sqrt{3} \times \sqrt{3}$)R30° structure

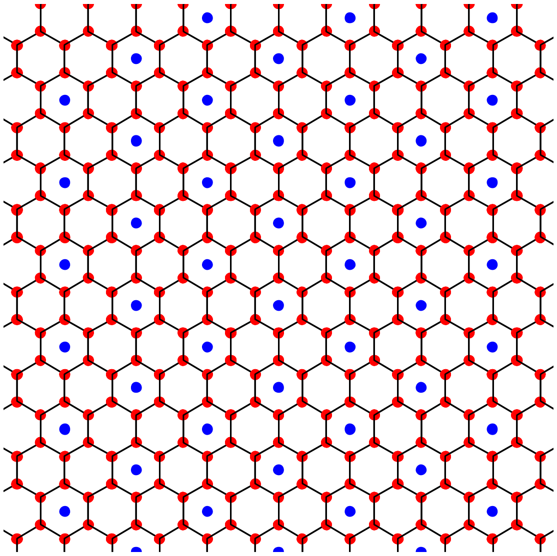

Fig. Schematic diagram of an in-plane unit cell for the p($\sqrt{3} \times \sqrt{3}$)R30° structure.

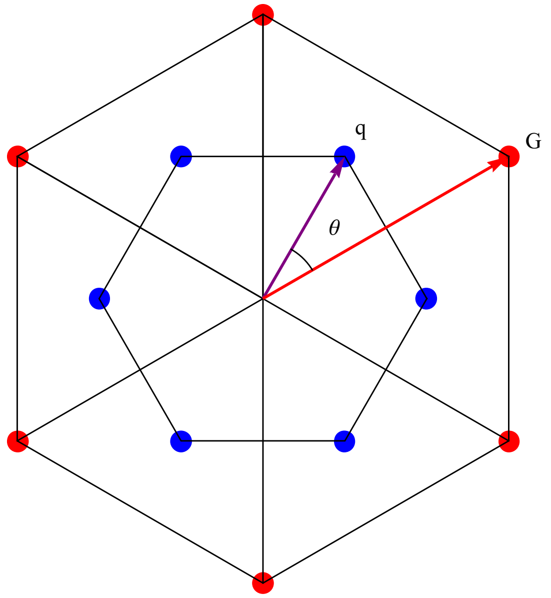

Fig. Bragg reflections arising from the graphite layer (red circles) and intercalate layer (blue circles) for the stoichiometry C_6M. The in-plane structure of the intercalate layer is p($\sqrt{3}\times\sqrt{3}$)R30°. $\boldsymbol{q}$ and G are the reciprocal lattice vectors of the graphite and intercalate layer, respectively. The rotation angle is θ= 30°. $\frac{|\mathbf{q}|}{|\mathbf{G}|}=\frac{1}{\sqrt{3}}$.

(iv) p($\sqrt{7}\times\sqrt{7}$)R19.11° structure

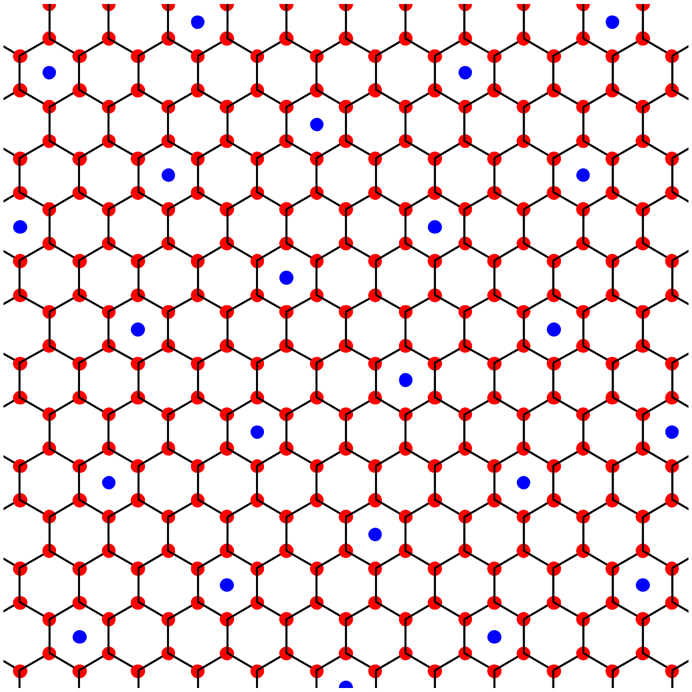

Fig. Schematic diagram of an in-plane unit cell for the p($\sqrt{7}\times\sqrt{7}$)R19.11° structure.

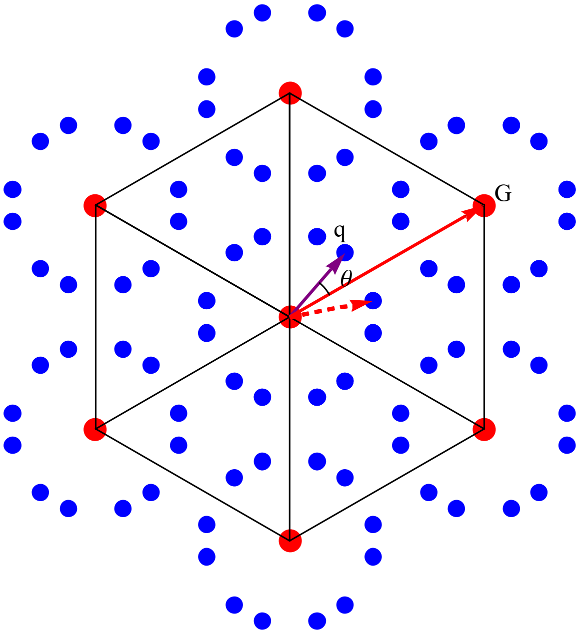

Fig. Bragg reflections arising from the graphite layer (red circles) and intercalate layer (blue circles) for the stoichiometry $C_{14}M$. The in-plane structure of the intercalate layer is p($\sqrt{7}\times\sqrt{7}$)R19.11°. $\boldsymbol{q}$ and G are the reciprocal lattice vectors of the graphite and intercalate layer, respectively. There are two kinds of domains with the rotation angle $\theta = \pm 19.11°$ for the $\frac{|\mathbf{q}|}{|\mathbf{G}|} = \frac{1}{\sqrt{7}}$.

9. Example: five-fold symmetry of quasi-crystal

Electron diffraction pattern of Al-Fe-Cu quasi crystal, which show clear five-fold symmetry.

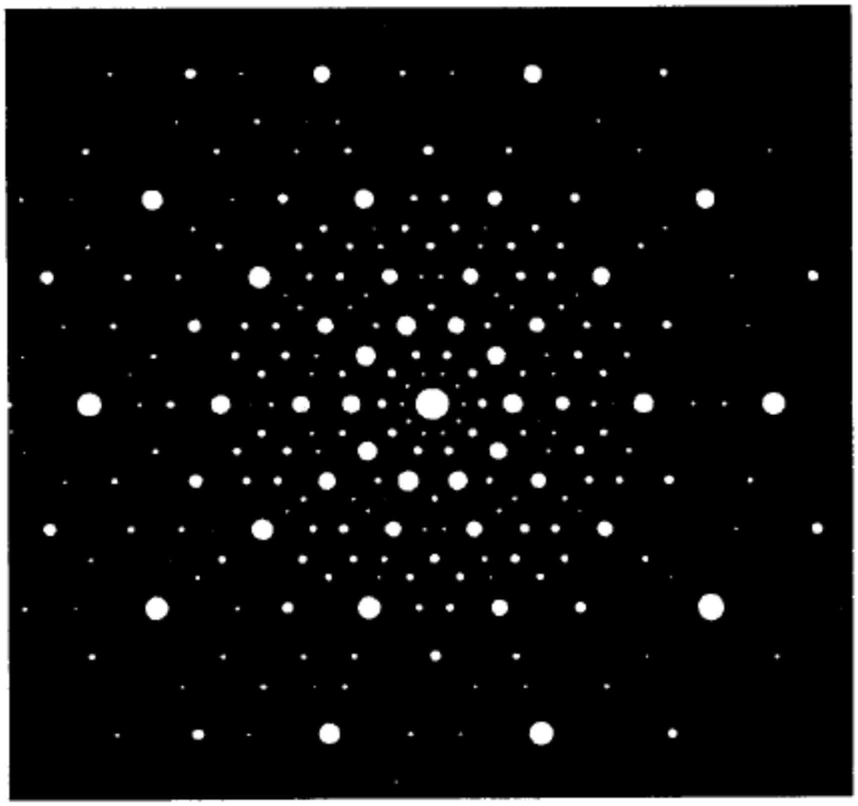

Fig. Electron diffraction pattern of quasi crystal Al-Fe-Cu (by K. Hiraga, Science 1990, September issue, p.54 (Japanese journal)]

APPENDIX-I

Wavelength of electrons as a function of the kinetic energy *K* (keV)

K(keV)	$\lambda_{\text{classical}}$(A)	$\lambda_{\text{relativistic}}$(A)
0.01	3.87831	3.87828
0.02	2.74238	2.74234
0.03	2.23914	2.2391
0.04	1.93916	1.93911
0.05	1.73443	1.73439
0.06	1.58331	1.58326
0.07	1.46586	1.46581
0.08	1.37119	1.37113
0.09	1.29277	1.29271
0.1	1.22643	1.22637

K(keV)	$\lambda_{\text{classical}}$(A)	$\lambda_{\text{relativistic}}$(A)
0.1	1.22643	1.22637
0.2	0.867217	0.867129
0.3	0.70808	0.707973
0.4	0.613215	0.613093
0.5	0.548476	0.54834
0.6	0.500688	0.500539
0.7	0.463547	0.463387
0.8	0.433608	0.433437
0.9	0.40881	0.408629
1.	0.387831	0.38764

K(keV)	$\lambda_{\text{classical}}$(A)	$\lambda_{\text{relativistic}}$(A)
1	0.387831	0.38764
2	0.274238	0.273969
3	0.223914	0.223586
4	0.193916	0.193537
5	0.173443	0.17302
6	0.158331	0.157868
7	0.146586	0.146086
8	0.137119	0.136585
9	0.129277	0.128711
10	0.122643	0.122047

K(keV)	$\lambda_{classical}$ (A)	$\lambda_{relativistic}$ (A)
10	0.122643	0.122047
20	0.0867217	0.0858851
30	0.070808	0.0697908
40	0.0613215	0.0601554
50	0.0548476	0.0535531
60	0.0500688	0.0486606
70	0.0463547	0.0448442
80	0.0433608	0.0417572
90	0.040881	0.0391916
100	0.0387831	0.0370144

K(keV)	$\lambda_{classical}$ (A)	$\lambda_{relativistic}$ (A)
100	0.0387831	0.0370144
200	0.0274238	0.0250793
300	0.0223914	0.0196875
400	0.0193916	0.0164394
500	0.0173443	0.0142126
600	0.0158331	0.012568
700	0.0146586	0.0112928
800	0.0137119	0.0102695
900	0.0129277	0.00942689
1000	0.0122643	0.00871919

APPENDIX-II: Understanding of the Davisson-Germer experiment (M. Suzuki and I.S. Suzuki)

https://arxiv.org/pdf/1307.6049.pdf

(1). INTRODUCTION

The observation of diffraction and interference of electron waves would provide the crucial test of the existence of wave nature of electrons. This observation was first seen in 1927 by C. J. Davisson and L. H. Germer.[1] They studied electron scattering from a target consisting of a single crystal of nickel (Ni) and investigated this phenomenon extensively. Electrons from an electron gun are directed at a crystal and detected at some angle that can be varied. For a typical pattern observed, there is a strong scattering maximum at an angle of 50°. The angle for maximum scattering of waves from a crystal depends on the wavelength of the waves and the spacing of the atoms in the crystal. Using the known spacing of atoms in their crystal, they calculated the wavelength that could produce such a maximum and found that it agreed with the de Broglie equation for the electron energy they were using. By varying the energy of the incident electrons, they could vary the electron wavelengths and produce maxima and minima at different locations in the diffraction patterns. In all cases, the measured wavelengths agreed with de Broglie's hypothesis.

The **Davisson-Germer experiment** itself is an established experiments. There is no controversy for them. How about the physical interpretation? One can see the description of the experiments and its physical interpretation in any standard textbook of the modern physics, which is one of the required classes for the physics majors (undergraduate). Nevertheless, students as well as instructors in this course may have some difficulty in understanding the underlying physics, since the descriptions of the experiments are different depending on textbooks and are not always specific.

As far as we know, proper understanding has not been achieved fully so far. In some textbooks, the Ni layers are thought to act as a reflective diffraction grating. When electrons are scattered by the Ni (111) surface (single crystal), the electrons strongly interact with electrons inside the system. Thus electrons are scattered by a Ni single layer. The Ni (111) surface is just the two-dimensional layer for electrons. The 2D character of the scattering of electrons appears in the form of a Bragg rod (or Bragg ridge) in the reciprocal lattice space. In other textbooks, electrons are scattered by Ni layers which acts as a bulk system. The 3D character of the scattering of electrons appears in the form of a Bragg points in the reciprocal lattice space.[13-18] The 3D Bragg reflection can occur when the Bragg points lie on the surface of Ewald sphere, like the x-ray diffraction.

Here we will show that the Ni layers acts as a reflective diffraction grating. The 2D scattering of electrons on the Ni (111), Ni(100), and Ni(110) surfaces will be discussed in terms of the concept of the Bragg rod (or Bragg ridge) which intersects the surface of the Ewald sphere. We will show that the experimental results[1-5]obtained by Davisson and Germer can be well explained in terms of our model.

(2) MODEL: EWALD SPHERE AND 2D BRAGG SCATTERING

In 1925, Clinton Davisson and Lester .H. Germer investigated the properties of Ni metallic surfaces by scattering electrons. Their experiments (Davisson-Germer experiment) demonstrates the validity of de Broglie's postulate because it can only be explained as a constructive interference of waves scattered by the periodic arrangement of the atoms of the crystal. The Bragg law for the diffraction had been applied to the x-ray diffraction, but this was first application to the electron waves.

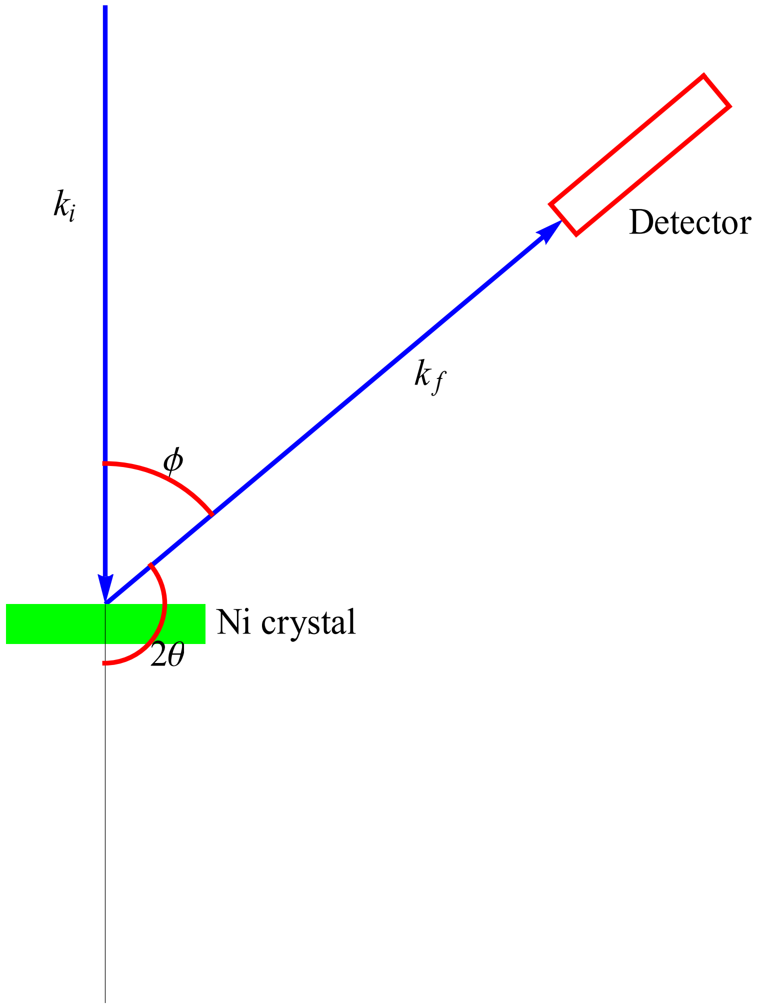

Fig. Constructive interference of electron waves scattered from a single layer of Ni atoms at an angle ϕ.

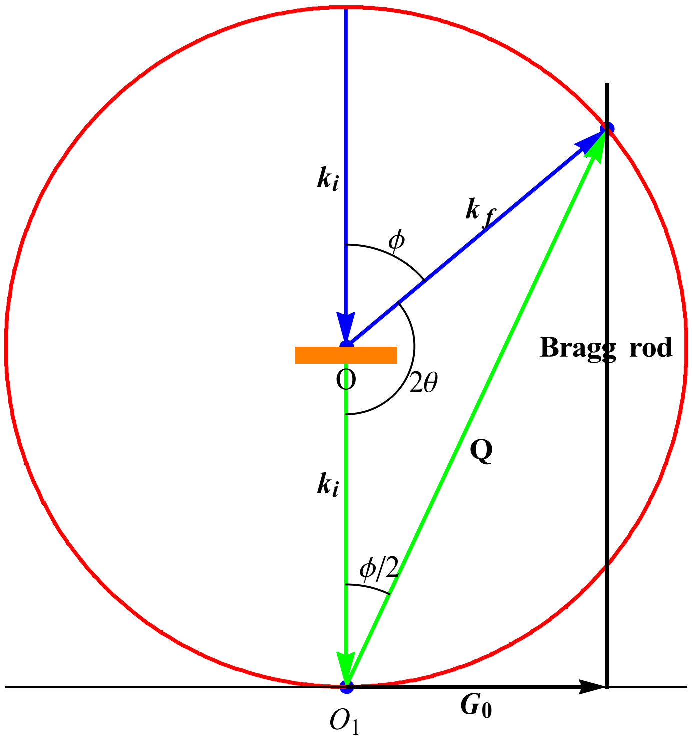

Fig. Ewald sphere for the Bragg reflection for the 2D system. The wavevector k_i is drawn in the direction of the incident electron beam. Ewald sphere (radius ($k_f = k_i = \frac{2\pi}{\lambda_{rel}}$) is centered at the point O The point O_1 is the origin of the reciprocal lattice vectors. The Bragg reflection occurs when the surface of the Ewald sphere intersects the Bragg rod originated from the nature of the 2D system: $\phi = 50°$. $K = 54$ eV. $\lambda_{rel} = 1.66891$ Å for the Ni(111) plane. The lattice constant of fcc Ni is $a = 3.52$ Å.

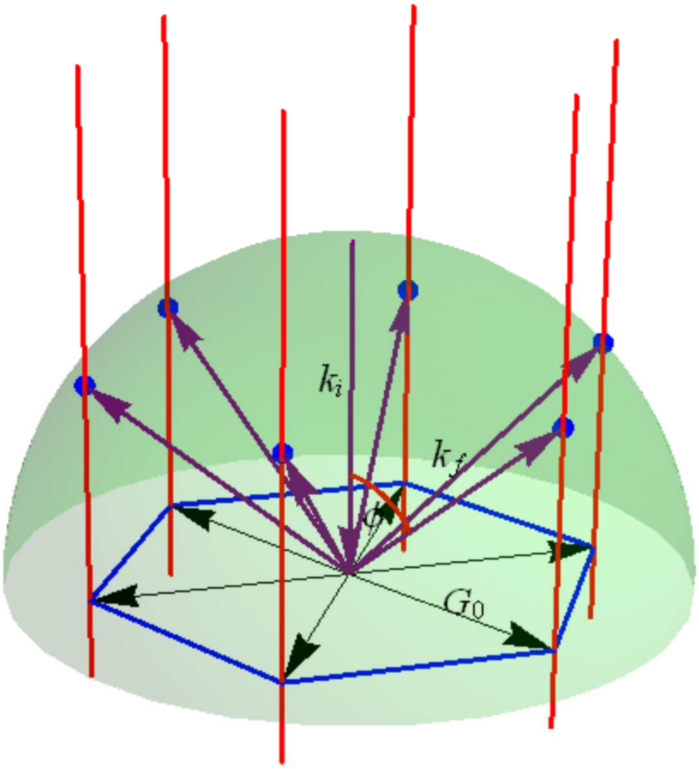

Fig. Ewald sphere for the two-dimensional layer with the radius $\left|\boldsymbol{k}_i\right| = \left|\boldsymbol{k}_f\right| = \frac{2\pi}{\lambda_{rel}}$. The red lines are denoted by the Bragg rods arisen from the character of the 2D system. The Bragg reflection occurs when the wave vector of the reflected wave is on the point (denoted by the blue points, which are not the Bragg points), where the Ewald sphere intersects the Bragg rod.

We now consider the Bragg reflections in the 2D system. These Bragg reflections occurs along the reciprocal rod in the reciprocal lattice space. The Bragg peaks appear along the reciprocal rod, which is described by ($\mathbf{G}_{\perp}$, $G_{//}$). Note that $\mathbf{G}_{\perp}$ is the in-plane reciprocal lattice vector and $G_{//}$ is the out-of-plane wavevector. The incident electron wave ($\boldsymbol{k}_{\mathrm{i}} = \boldsymbol{k}$, $k = 2\pi/\lambda_{rel}$) is reflected by the surface of the 2D system. $\boldsymbol{k}_{\mathrm{f}}$ (= $\boldsymbol{k}'$) is the wavevector of the out-going electron wave ($k' = 2\pi/\lambda_{\mathrm{rel}}$).

Here we use the notation λ_{rel} as the wavelength, instead of the conventional notation λ. The Ewald sphere is formed of the sphere with the radius of $k = k'$. The scattering vector $\boldsymbol{Q}$ is defined by

$$\boldsymbol{Q} = \boldsymbol{k}' - \boldsymbol{k} . \qquad (1)$$

O$_1$ is the origin of the reciprocal lattice space. The 2D system is located at the point O. The direction normal to the surface of the system is anti-parallel to the direction of the incident electron wave. Since the system is two-dimensional, the reciprocal lattice space is formed of Bragg rods. The Bragg reflections occur when the Bragg rods intersect the Ewald sphere.

Because of the 2D system, the Bragg points of the 3D system are changed into the Bragg rods. Then the Bragg condition occurs under the condition,

$$k' \sin\phi = G_0 , \qquad (2)$$

where

$$k = k' = \frac{2\pi}{\lambda_{rel}} . \qquad (3)$$

The scattering angle 2θ is related to the angle f as

$$\phi = \pi - 2\theta . \qquad (4)$$

In the electron diffraction experiment, we usually need to use the wavelength (λ_{rel}), which is taken into account of the special relativity,[7-12]

$$\sin(\pi - 2\theta) = \frac{G_0}{k'} = \frac{G_0}{2\pi}\lambda_{rel} , \qquad (5)$$

or

$$\sin(2\theta) = \frac{G_0}{2\pi}\lambda_{rel}, \tag{6}$$

where λ_{rel} is the wavelength,

$$\lambda_{rel} = \frac{\frac{hc}{E_0}}{\sqrt{\frac{K}{E_0}\left(\frac{K}{E_0}+2\right)}}. \tag{7}$$

where h is the Plank's constant and c is the velocity of light, K (in the units of eV) is the kinetic energy of electron. E_0 (= mc^2) is the rest energy. In the non-relativistic limit, we have

$$\lambda_{classical} = \frac{12.2643}{\sqrt{K(eV)}}\text{Å}. \tag{8}$$

in the unit of Å. When K = 54 eV, λ is calculated as λ = 1.66891 Å.

Suppose that Ni (111) plane behaves like a three-dimensional system. The 3D Bragg reflection occurs only if the Bragg condition

$$\boldsymbol{Q} = \boldsymbol{k}_f - \boldsymbol{k}_i = \boldsymbol{G}, \tag{9}$$

is satisfied, where $\boldsymbol{Q}$ is the scattering vector and $\boldsymbol{G}$ is the reciprocal lattice vectors for the 3D system. In the experimental configuration as shown in Fig.2. G is one of the reciprocal lattice vectors for the fcc Ni and appears in the form of Bragg point. This Bragg point should be located on the surface of the Ewald sphere with radius ($k_f = k_i = \frac{2\pi}{\lambda_{rel}}$) centered at the point O (see Fig.2). No existence of such a Bragg point on the Ewald sphere indicates that the 3D Bragg scattering does not occur in the present situation.

APPENDIX II Heisenberg's explanation for the Davisson-Germer experiment

The physical meaning of the Davisson-Germer experiment was discussed by Werner Heisenberg in his famous book, [W. Heisenberg, The Physical Principles of the Quantum Theory, translated by C. Eckart and F.C. Hoyt (Dover, 1949)]. In the Germany version of this book, the diffraction grating is used to explain the Davisson-Germer experiment. Unfortunately, such an important figure is removed in the English version.

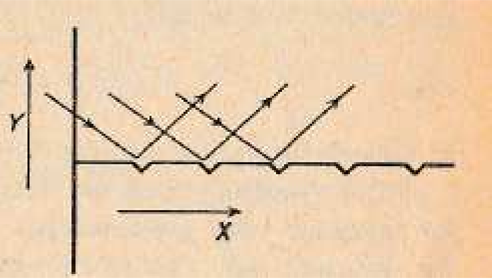

The diffraction of light or matter (Davisson-Germer, Thomson, Rupp, Kikuchi) by gratings may be explained most simply by the aid of the classical wave theories. The application of space-time wave theories to these experiments is justified from the point of view of the quantum theory, since the uncertainty relations do not in any way affect the purely geometrical aspects of the waves, but only their amplitude. The quantum theory needs only be invoked when discussing the dynamical relations involving the energy and momentum content of the waves.

The quantum theory of the waves being thus certainly in agreement with the classical theory in so far as the geometric diffraction pattern is concerned, it seems useless to prove it by detailed calculation. On the other hand, Duane has given an interesting treatment of diffraction phenomena from the quantum theory of the corpuscular picture. We imagine for simplicity that the corpuscle is reflected from a plane ruled grating, whose constant is d.

Let the grating itself be movable. Its translation in the x-direction may be looked upon as a periodic motion, in so far as only the interaction of the incident particles with the grating is considered; for the displacement of the whole grating by an amount d will not change this interaction. Thus we may conclude that the motion of the grating in this direction is quantized and that its momentum p_x may assume only the values nh/d (as follows at once from the earlier form of the theory: $\int pdq = nh$). Since the total momentum of grating and particle must remain unchanged, the momentum of the particle can be changed only by an amount mh/d (m an integer):

$$p_x' = p_x + \frac{mh}{d}.$$

Furthermore, because of its large mass, the grating cannot take up any appreciable amount of energy, so that

$${p_x'}^2 + {p_y'}^2 = p_x^2 + p_y^2 = p^2.$$

If θ is the angle of incidence, θ' that of reflection, we have

$$\cos\theta = \frac{p_y}{p}, \qquad \cos\theta' = \frac{p_{y'}}{p},$$

whence

$$\sin\theta' - \sin\theta = \frac{mh}{pd}.$$

From the de Broglie relation for the wave-length of the wave associated with a particle it then follows that

$$d(\sin\theta' - \sin\theta) = \frac{mh}{p} = m\lambda$$

in agreement with the ordinary wave theory.

APPENDIX-III Ewald construction for the 2D system: existence of Bragg rod

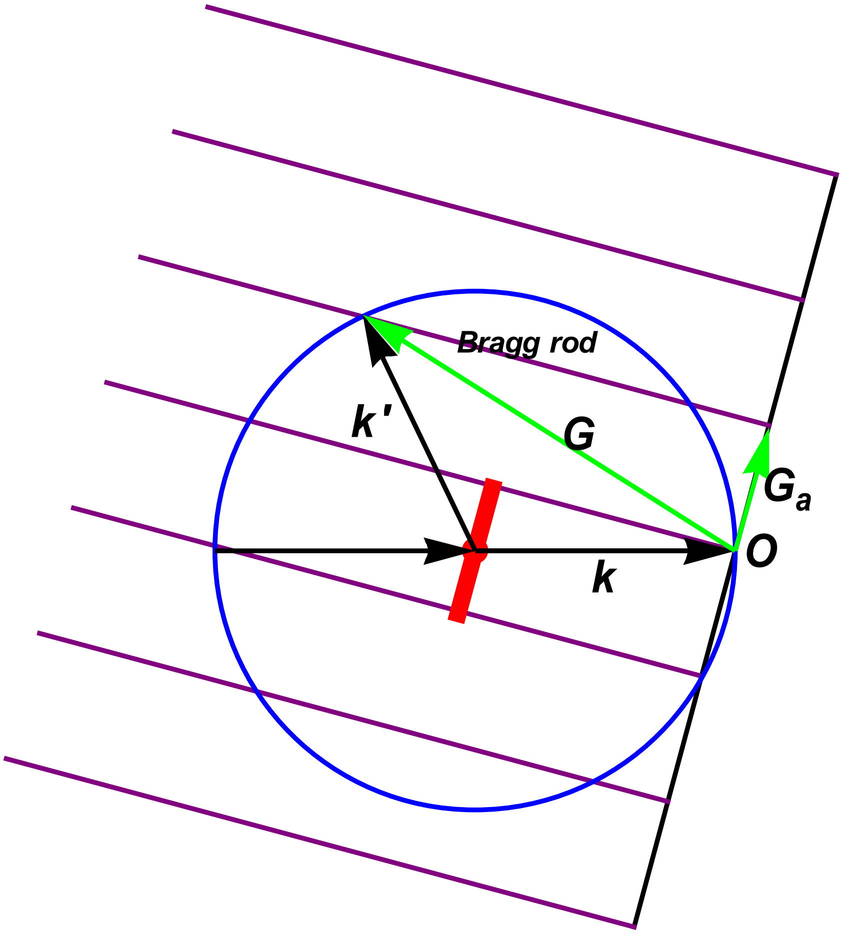

Fig. Ewald construction for elastic scattering on a 2D surface lattice. The Bragg condition is satisfied when the in-plane component of the scattering vector $\boldsymbol{Q} = \boldsymbol{k}' - \boldsymbol{k}$ is equal to the in-plane reciprocal lattice vector.

In the 2D case, the possible elastically scattered beams (k') can be obtained by the Ewald construction. The wave vector k of the incident beam is positioned with its end at the (0,0) reciprocal lattice point and a sphere is constructed around its starting point. As is seen from Fig, the condition $Q_a = G_a$ is fulfilled for every point at which the sphere crosses a reciprocal lattice rod.

APPENDIX-IV Reciprocal lattice vector of fcc plane

Copper is a metal with the fcc structure. Suppose a Cu layer located on the surface of the single crystal [Cu(100) layer. Cu(110) layer, and Cu(111) layer]. The Bragg rod arising from the nature of the two dimensionality is formed on the reciprocal lattice plane.

(a) Bragg rod for the (100) plane

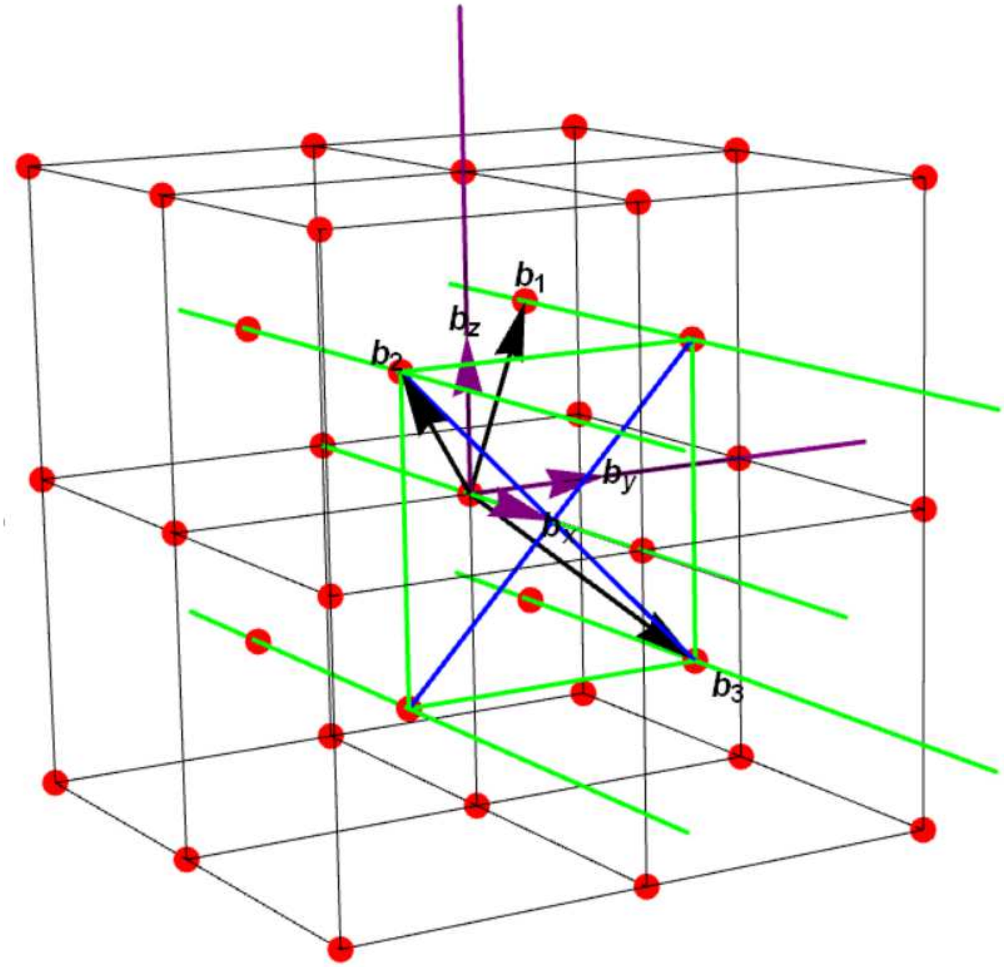
b_1
b_z
b_2
b_y
b_x
b_3

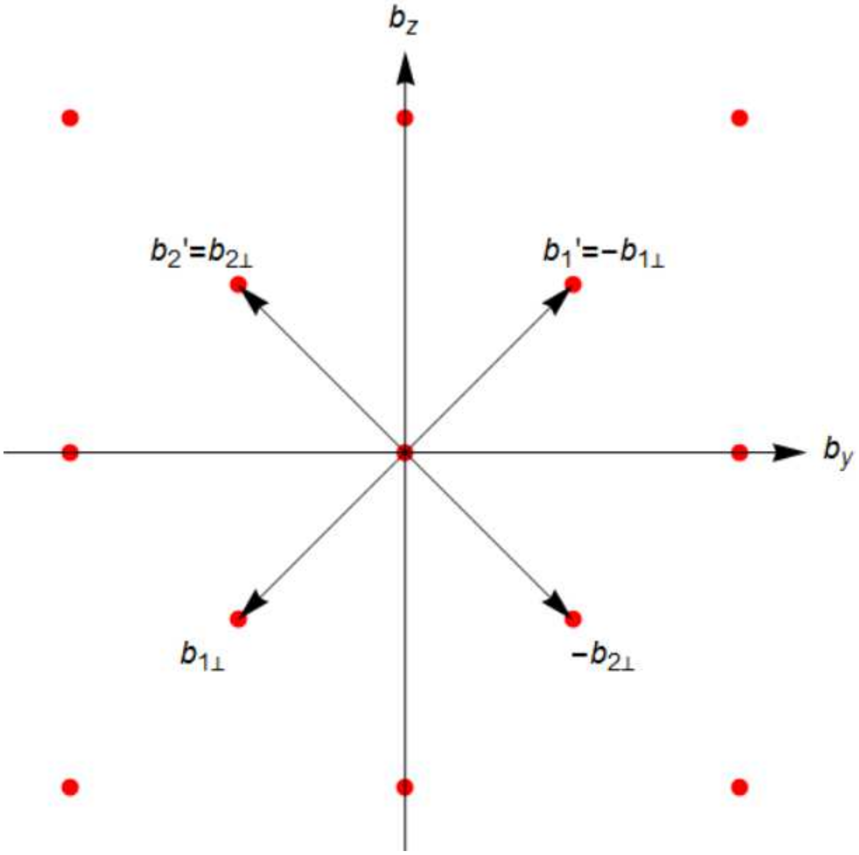

(b) **Bragg rod for the (111) plane**

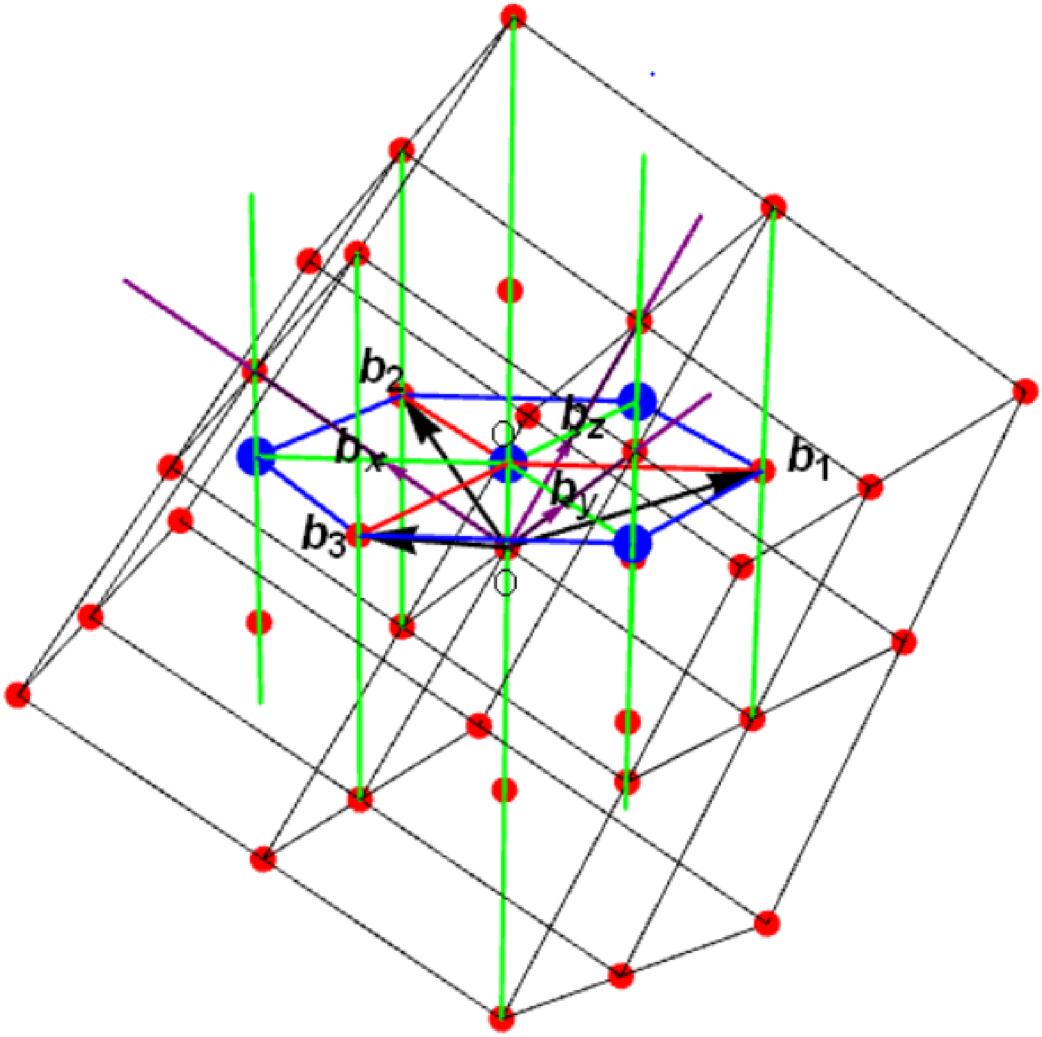
b_2
b_z
b_x
b_1
b_y
b_3

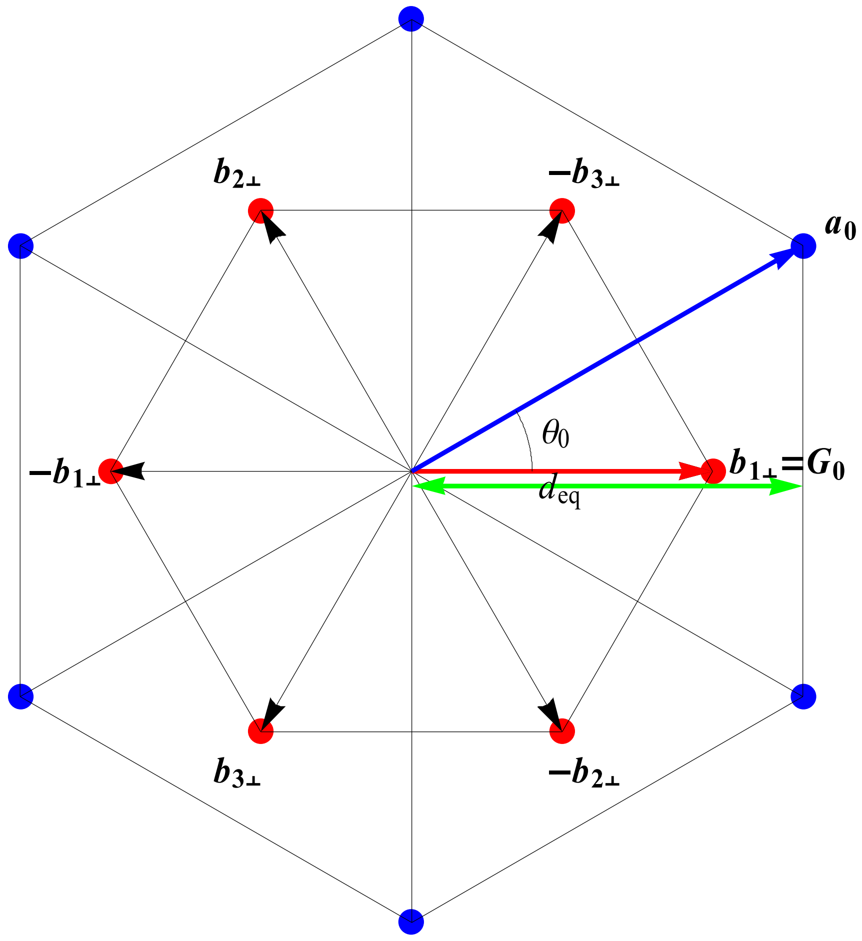

(c) Bragg rod for the (110) plane

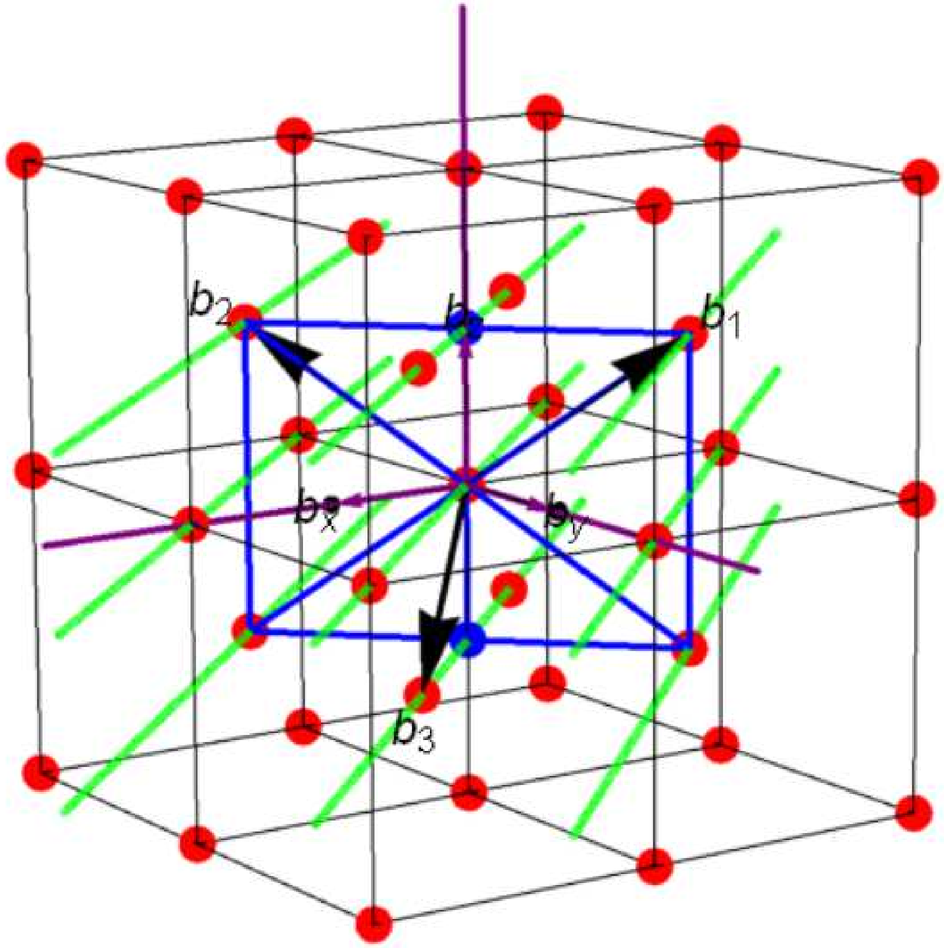
b_2
b
b_1
b_x
b_y
b_3

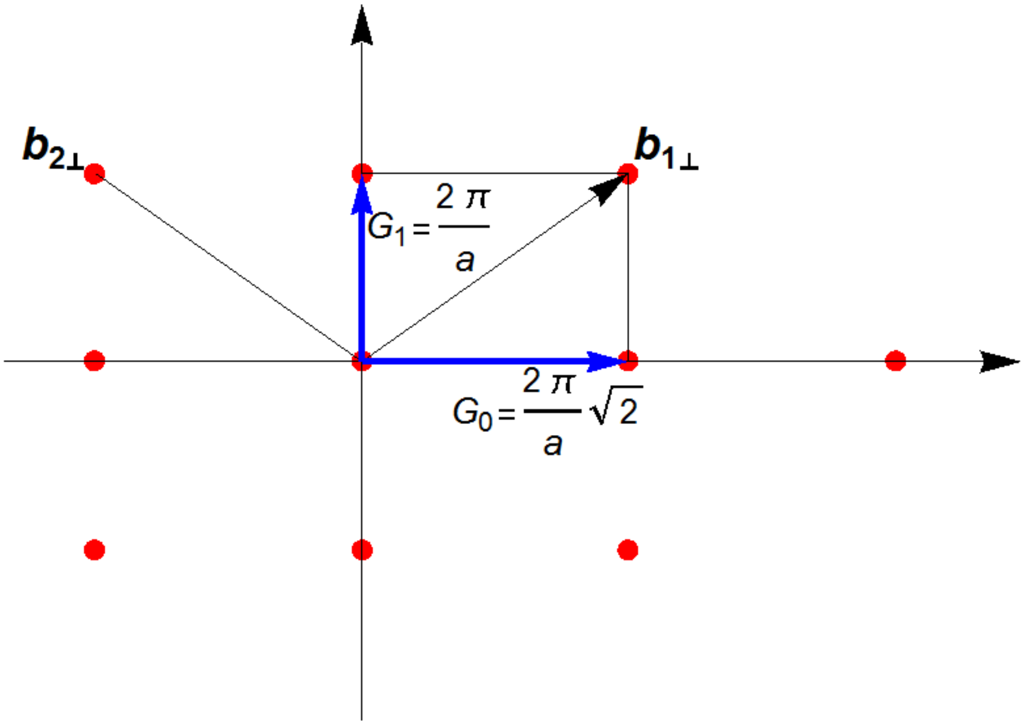

((In summary))

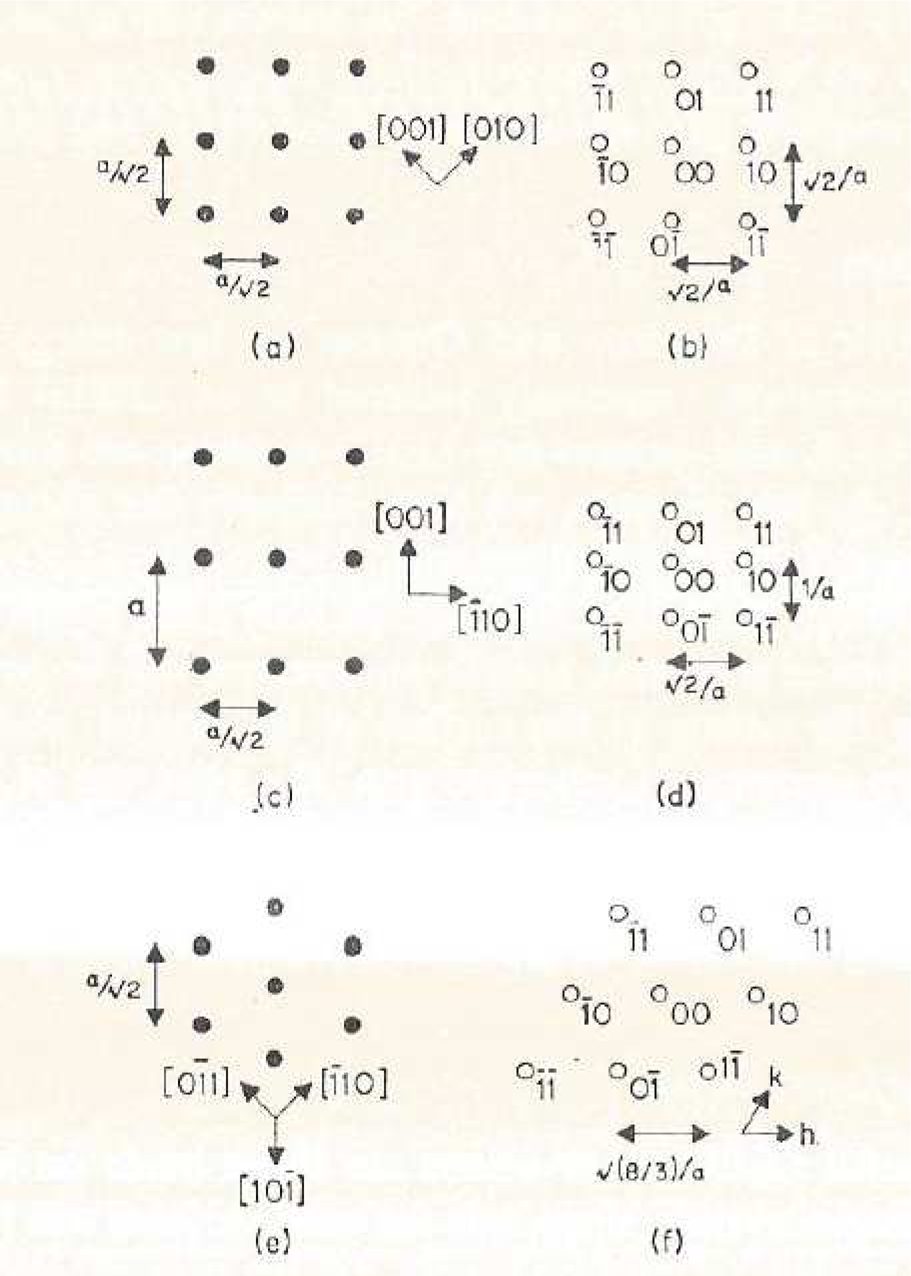

Fig. LEED (low energy electron diffraction) patterns from fcc crystal. The solid discs represent atoms in the surface of the crystal, the open circles represent reciprocal lattice points corresponding to these surface planes of atoms (T.D. Rymer, Electron Diffraction (Methuen Co Ltd, 1970).

(a) Arrangement of atoms in (100) face.
(b) Reciprocal lattice corresponding to (a)
(c) Arrangement of atoms in (110) face.
(d) Reciprocal lattice corresponding to (c)

(e) Arrangement of atoms in (111) face.
(f) Reciprocal lattice corresponding to (e)

REFERENCES

T.D. Rymer, Electron Diffraction (Methuen Co Ltd, 1970).

L.J. Clarke, *Surface Crystallography An Introduction to Low Energy Electron Diffraction* (John Wiley & Sons, New York, 1985).

J. Als-Nielsen and D. McMorrow, *Elements of Modern x-ray Physics* (John Wiley & Sons, Ltd., New York, 2001).

H. Lüth, Solid Surfaces, *Interfaces and Thin Films*, fourth, revised and extended edition (Springer, Berlin, 2001).

J.M. Cowley, *Diffraction Physics*, third revised edition (Elsevier Science B.V., Amsterdam, 1995).

W. Heisenberg, Die Physikalischen, Prinzipien der Quantumtheorie (Biblographisches Institut AG, 1958).

W. Heisenberg, The Physical Principles of the Quantum Theory, translated by C. Eckart and F.C. Hoyt (Dover, 1949).